p27^{kip1} haploinsufficiency preserves myocardial function in the early stages of myocardial infarction via Atg5-mediated autophagy flux restoration

NINGTIAN ZHOU[1*], QIONG HUANG[1*], WEILI CHENG[2], YINGBIN GE[3], DIANFU LI[1] and JUNHONG WANG[1]

[1]Department of Cardiology, The First Affiliated Hospital of Nanjing Medical University;
[2]Department of Cardiology, Jiangning Hospital of Nanjing Medical University;
[3]Department of Physiology, Nanjing Medical University, Nanjing, Jiangsu 210000, P.R. China

Received February 16, 2019; Accepted July 25, 2019

DOI: 10.3892/mmr.2019.10632

Abstract. Myocardial infarction (MI) is a leading cause of mortality in adults worldwide. Over the last two decades, gene therapy has been a hot topic in cardiology, and there has been a focus on cell cycle inhibitors and their protective effects on the myocardium post-MI. In our previous study, the haploinsufficiency of p27^{kip1} (p27) was demonstrated to improve cardiac function in mice post-MI by promoting angiogenesis and myocardium protection through the secretion of growth factors. Autophagy is an adaptive response of cells to environmental changes, such as nutrient deprivation, ischemia and hypoxia. The appropriate regulation of autophagy may improve myocardial function by preventing apoptosis of cardiomyocytes. In this study, we used immunoassays, transmission electron microscopy and cardiac ultrasound to confirm that p27 haploinsufficiency prevents myocardial apoptosis by restoring autophagy protein 5-mediated autophagy flux in the early stages of MI. The present study provides a novel method for studying MI or ischemic heart disease therapy.

Introduction

Myocardial infarction (MI) is a disease with the highest mortality rate, accounting for 1 in 5 deaths in the United States (1); in the past decade, 17.6 million individuals have suffered from MI. According to the American Heart Association, acute cardiac vascular occlusion and poor prognosis are the main causes of mortality (2). At present, instantly restoring blood flow to the ischemic area by percutaneous coronary intervention is the best approach to saving lives (3). Along with the development of gene technology and molecular biology, research into gene and genomic regulation is being conducted to reveal the cause of MI and to advance therapies (4). Cytokine and gene therapy have been widely utilized for therapeutic angiogenesis in myocardial ischemia (4). Various growth factors, such as vascular endothelial growth factor (VEGF) and hepatocyte growth factor (HGF), serve roles in balancing cell proliferation and survival under stress (5-7). Furthermore, cardiac remodeling and collateral angiogenesis improve early cardiac recovery (8). In our previous study, it was reported that p27^{kip1} (p27) haploinsufficiency improved cardiac function in the early stages of MI by protecting the myocardium and increasing angiogenesis through IκB kinase activation (9). The protective effects of knocking down the cell cycle inhibitor p27 to stimulate the autocrine and paracrine effects of VEGF and HGF through the activation of inflammation and angiogenesis in the myocardium.

p27 is a potent cell cycle inhibitor that maintains cell proliferation by arresting the cell cycle in the G0/G1 phase; a previous study reported that the regulation of p27 not only affected cell cycle-related proliferation but was also involved in multifunctional molecular mechanisms *in vivo* and *in vitro* such as aging and inflammation regulating (10). The downstream activities of p27 include the regulation of inflammation and survival pathways (9,11,12). Through the regulation of p27 expression, development/tumorigenesis and metabolism are altered, which are implicated in energy modulation (13). Rossi *et al* (14) reported that gene knockdown may induce different biological effects than gene deletion; it was found that knockdown was more effective than knockout for mimicking pathological progression. In our previous study, p27 haploinsufficient mice (p27$^{+/-}$) exhibited a different phenotype compared with wild-type (WT; p27$^{+/+}$) or homozygous (p27$^{-/-}$) mice (9).

Macroautophagy, more commonly referred to as autophagy, balances cell death and survival in response to stress and starvation (15). It is an important cellular homeostatic

Correspondence to: Professor Dianfu Li or Dr Ningtian Zhou, Department of Cardiology, The First Affiliated Hospital of Nanjing Medical University, 300 Guangzhou Road, Nanjing, Jiangsu 210000, P.R. China
E-mail: callsky1986@aliyun.com
E-mail: lidianfu@jsph.org.cn

*Contributed equally

Key words: p27^{kip1}, myocardial infarction, apoptosis, autophagy

process that cells use to degrade misfolded proteins and recycle damaged organelles, and is also related to a number of diseases, including cancer and neurodegeneration. The cup-shaped pre-autophagosomal double-membrane structure containing cytoplasmic material characterizes the formation of autophagosomes (16). As previously reported, the cardiomyocyte-specific abrogation of basal autophagy that results from a deficiency in autophagy protein 5 (Atg5) leads to spontaneous cardiac hypertrophy (17). Accordingly, autophagy acts as a protective mechanism that improves cardiomyocyte survival under stress (18). Serum withdrawal and hypoxia are common approaches used to mimic myocardial cell ischemia *in vitro*. Ding *et al* (19) reported that p27 levels were regulated by autophagy in serum-deprived mouse mesangial cells. It also has been reported that, in relation to autophagy and inflammation, cardiac remodeling and heart failure are promoted by the upregulation of p27 in the long term (20). To the best of our knowledge, no studies have investigated the relationship between p27 and autophagy in the early stages of MI.

The present study aimed to determine the functional role of p27 haploinsufficiency in the induction of autophagy by hypoxia and serum withdrawal *in vitro* and *in vivo* for cardiomyocyte survival, and protection from apoptosis. The results demonstrated that $p27^{+/-}$ resulted in the increased induction of Atg5-related autophagosomes and suppressed serum withdrawal-induced caspase-3 activation and apoptosis in MI hearts. It was demonstrated that p27 knockdown governed the regulation of autophagy by increasing the expression of Atg5 in the early stages of MI in mice and in MI mimic cells. In the present study, 3-methyladenine (3-MA) and rapamycin were used to investigate the rescue of autophagy and cell survival following MI.

Materials and methods

Animals and establishment of an MI model. The establishment of the MI animal model was described in our previous study (9). $p27^{+/-}$ and strain-specific C57BL/6 WT $p27^{+/+}$ mice were bred from a breeding pair of heterozygous p27 mice (kindly donated by Professor Dengshun Miao, McGill University; Fig. S1A) and housed in the Animal Research Center of Nanjing Medical University. The mice were bred in a specific pathogen-free rodent feeding room and kept at 15% humidity and 25˚C conditions and a 12 h-light/dark cycle. Tail fragment genomic DNA was used to genotype the mice; a total of 40 adult male 3-month-old C57BL/6 (25±5 g) WT (n=20) and $p27^{+/-}$ (n=20) mice were split into MI and Sham control groups (10 mice/group). Left anterior descending (LAD) artery ligation was performed to induce MI, as previously describe (9). Briefly, the LAD coronary artery was ligated permanently using an 8-0 polypropylene suture; the Sham animals underwent the same procedure, but without ligation of the LAD coronary artery. During the experimental trial, all mice were allowed *ad libitum* access to food and water. The protocols used in the present study were approved by the Ethics Review of Lab Animal Use Application of Nanjing Medical University, and the procedures complied with the National Institutes of Health Guide for the Care and Use of Laboratory Animals (9).

Echocardiogram. Cardiac function was determined using a high-frequency ultrasound system Vevo2100 (FUJIFILM VisualSonics, Inc.) equipped with a 30-MHz transducer. The ejection fraction (EF) and fractional shortening (FS) were calculated according to the following formulas: EF=[(LVEDV-LVESV)/LVEDV] x100, where LVEDV is left ventricular end-diastolic volume and ESV is LV end-systolic volume; and FS=[(LVEDd-LVESd)/LVEDd] x100, where EDd is end-diastolic dimension and ESd is end-systolic dimension. Each parameter was the average of three values. Mice were anesthetized with 4-5% chloral hydrate at 300-4550 mg/kg; no signs of peritonitis, pain or discomfort were observed. The heart rates of the mice were maintained at 250±35 beats/min under anesthesia.

Immunohistochemistry (IHC) and Masson's trichrome staining. Mouse hearts were collected and left ventricular tissues fixed in 4% buffered paraformaldehyde at room temperature for 24 h and embedded in paraffin at 60˚C for 1 h. The paraffin embedded tissues were cut into 5 μm-thick sections, which were subsequently deparaffinized and rehydrated with a graded xylene and ethanol series. Antigen retrieval was performed by high temperature and pressure: 1 mM EDTA (Beijing Solarbio Science & Technology Co., Ltd.) was heated to 100˚C, the sections were soaked in EDTA and heated for 5 min at a pressure of 110 kPa. Sections were incubated in 3% H_2O_2 at room temperature for 10 min. Subsequently, the sections were blocked in 10% BSA (Beijing Solarbio Science & Technology Co., Ltd.) at room temperature for 30 min. IHC was performed using the SuperPicture™ 3rd Gen IHC Detection kit (cat. no. 878973; Invitrogen; Thermo Fisher Scientific, Inc.), following manufacturer's protocol. Briefly, the sections were incubated with a primary antibody against microtubule-associated proteins 1A/1B light chain (LC3) (1:500; cat. no. ab128025; Abcam) overnight at 4˚C. The sections were subsequently incubated with a horseradish peroxidase (HRP)-conjugated goat anti-rabbit secondary antibody [1:500: cat. no. 7074/6; Cell Signaling Technology, Inc. (CST)] for 2 h at 25˚C. A two-step technique was used for visualization using components from the SuperPicture™ 3rd Gen IHC Detection kit, and hematoxylin was used as a counterstain. The heart tissue sections from the left ventricle of mice 28 days post-MI and fixed, embedded, cut into 5-μm-thick sections were also stained using Masson's trichrome to confirm successful model establishment by infarction and fibrotic areas (Fig. S1B). A total of six fields were analyzed per sample and images were captures using an Olympus CX41 light microscope (CX41; Olympus Corporation, Tokyo, Japan) and Image-Pro Plus 6.0 (Media Cybernetics, Inc.) was used to detect LC3 expression.

Cell culture and treatment. The rat H9c2 cell line (cat. no. GNR5; Cell Bank of the Chinese Academy of Science) was seeded at $1.25x10^4$ cells/well in DMEM (Gibco; Thermo Fisher Scientific, Inc.) in 6-well culture plates and were allowed to grow for 2 days in incubated box at 37˚C, 5% CO_2, pH 7.2-7.4. FBS (10%; Gibco; Thermo Fisher Scientific, Inc.), 100 IU/ml penicillin and 100 μg/ml streptomycin were added to the culture medium before cell culture. When the cells reached 80-85% confluency the media was replaced with DMEM containing 1% FBS, to mimic ischemia, and the cells were placed into an anoxic box (95% nitrogen, 5% CO_2 at 37˚C)

to induce hypoxia for 3 or 12 h. Confirmation of hypoxia was determined by western blotting for increased protein expression levels of hypoxia-inducible factor-1α (HIF-1α; Fig. S1C).

Western blot analysis. Tissues and cells were lysed using RIPA buffer [20 mM Tris-HCl (pH 7.5), 150 mM NaCl, 1 mM Na_2EDTA, 1 mM EGTA, 1% NP-40, 1% sodium deoxycholate, 2.5 mM sodium pyrophosphate, 1 mM β-glycerophosphate, 1 mM Na_3VO_4, 1 μg/ml leupeptin]. Protein concentrations were determined by BCA; 20 μg of protein lysates were separated by 10% SDS-PAGE and transferred to PVDF membranes. Membranes were washed with PBS, blocked with 5% non-fat dry milk for 1 h at room temperature, and subsequently incubated over night at 4˚C with primary antibodies (all 1:1,000) against p27 (cat. no. 610241; BD Biosciences), Cleaved-caspase-3 (cat. no. 9664; CST), Bcl-2 (cat. no. 2870; CST), Beclin 1 (cat. no. 3495; CST), Atg5 (cat. no. 12994; CST), LC3 (cat. no. ab128025; Abcam), HIF-1α (cat. no. 36169; CST) and GAPDH (cat. no. 2118; CST). Subsequently, the membranes were incubated with HRP-conjugated goat anti-mouse (cat. no. sc-2005; Santa Cruz Biotechnology, Inc.) or goat anti-rabbit HRP (cat.no. sc-2004; Santa Cruz Biotechnology, Inc.) secondary antibodies overnight at 4˚C (both 1:2,000). Protein bands were visualized using the Tanon 4600 High-Sig ECL Western Blotting Substrate (Tanon Science and Technology Co., Ltd.) then Gel-Pro Analyzer 4.0 used for the densitometric analyses; GAPDH was used as a loading control and for normalization.

Cell transduction. Lentiviral vectors for pLV-$p27^{kip1}$-inhibitor (5'-AAGGTTGCATACTGAGCCAAG-3'), pLV-Atg5-inhibitor (5'-CAUCUGAGCUACCCGGAUAUU-3'), Scrambled shRNA negative control (NC) (5'-GGGTGATTCACTTTC AGGTCAGTAA-3') (all from Shanghai GeneChem Co., Ltd.) were used to establish stable knockdown cell lines (Fig. S1D). Briefly, $1x10^5$ H9c2 cells were incubated with lentiviruses (10 μg/ml; 20 multiplicity of infection) in the presence of 2 μg/ml polybrene (cat. no. sc-134220; Santa Cruz Biotechnology, Inc.) overnight at 37˚C. Stably transduced cells were selected using 2 μg/ml puromycin (Sigma-Aldrich; Merck KGaA).

Transmission electron microscopy (TEM). The tissues obtained from the ischemic area of the isolated hearts were cut into 1-2 mm^3 cubes and fixed with 2% glutaraldehyde in 0.1 M cacodylate buffer at 4˚C overnight. The excised tissues were embedded in epoxy resin, cut into 60-70-nm sections with an ultramicrotome and placed on TEM grids for examination using TEM at the public laboratory of Nanjing Medical University, gold was used to increase contrast for imaging.

Co-immunoprecipitation (Co-IP). Tissues were lysed in RIPA buffer, aforementioned, and incubated with primary antibodies (all 1:300) against Atg5 (cat. no. 12994; CST) and p27 (cat. no. 610241; BD Biosciences) and with protein G-agarose beads (cat. no. sc-2002; Santa Cruz Biotechnology, Inc.) overnight at 4˚C. The next day, beads were collected by centrifugation (4˚C; 3,000 x g; 5 min) and 60 μl of SDS sample buffer was used to wash the beads while heating at 100˚C for 10 min. The proteins collected were utilized for western blotting, following the aforementioned protocol.

Determination of apoptosis using flow cytometry. The level of apoptosis in the treated H9c2 cells was determined using an Annexin V-APC Apoptosis Detection kit (BD Biosciences) according to the manufacturer's instructions. The data were analyzed using a flow cytometer and Image-Pro Plus 6.0 used to analyze.

Autophagy detection using monomeric red fluorescent protein (mRFP)-green fluorescent protein (GFP) vector. H9c2 cells were plated in 6-well plates and allowed to reach a confluency of 70-85%. An mRFP-GFP-LC3 adenoviral vector (Hanbio Biotechnology Co., Ltd.) was used to infect the cells, according to the manufacturer's instructions. Cells were incubated in growth medium with the adenoviruses at a multiplicity of infection of 100 for 2 h at 37˚C. Cells were subsequently incubated in fresh medium for a further 24 h at 37˚C. After infection, cells were exposed to the aforementioned hypoxic/ischemic conditions for 3 h. Autophagy was observed using an Olympus BX51 fluorescent microscope (Olympus Corporation) as previously described (16).

Statistical analysis. Data are presented as the mean ± SEM from three independent experiments. All statistical analysis was conducted using SPSS 19.0 statistical software (IBM Corp.). Statistical significance between groups was determined using one-way ANOVA and Tukey's post hoc test. $P<0.05$ was considered to indicate a statistically significant difference.

Results

p27 haploinsufficiency improves cardiac function after MI. $p27^{+/-}$ has been shown to have either a proangiogenic or an antiapoptotic effect depending on cell cycle re-entry (9). LAD artery ligation was used to mimic MI in WT and $p27^{+/-}$ mice. In our previous study, it was reported that $p27^{-/-}$ and WT mice exhibited high mortality following this procedure, but that $p27^{+/-}$ mice had a moderate mortality (9). Significant systolic dysfunction was observed in WT MI compared with WT Sham ($P<0.05$), $p27^{+/-}$ MI compared with $p27^{+/-}$ Sham ($P<0.05$) at 28 days following MI and in WT MI compared with $p27^{+/-}$ MI as assessed using the percentage of LV FS and EF in the MI and control groups (Fig. 1A). However, LV dysfunction was lower in $p27^{+/-}$ mice compared with the WT mice after infarction ($P<0.05$; Fig. 1A). These data suggested that the haploinsufficiency of p27 may preserve cardiac function following MI. $p27^{+/-}$ mice exhibited reduced cardiac injury after MI by promoting the expression of the anti-apoptotic protein Bcl-2 at 3 days post-MI compared with WT MI at day 3 ($P<0.01$) and by reducing the protein expression level of cleaved caspase-3 at 3 and 28 days post-MI compared with the WT MI counterpart ($P<0.05$ and $P<0.01$, respectively) (Fig. 1B and C).

p27 haploinsufficiency attenuates ischemic injury through a pro-autophagy-induced antiapoptotic pathway in vivo. As shown in Fig. 2A, MI induced the expression of the autophagic vesicle-associated form of LC3-II within 28 days after LAD

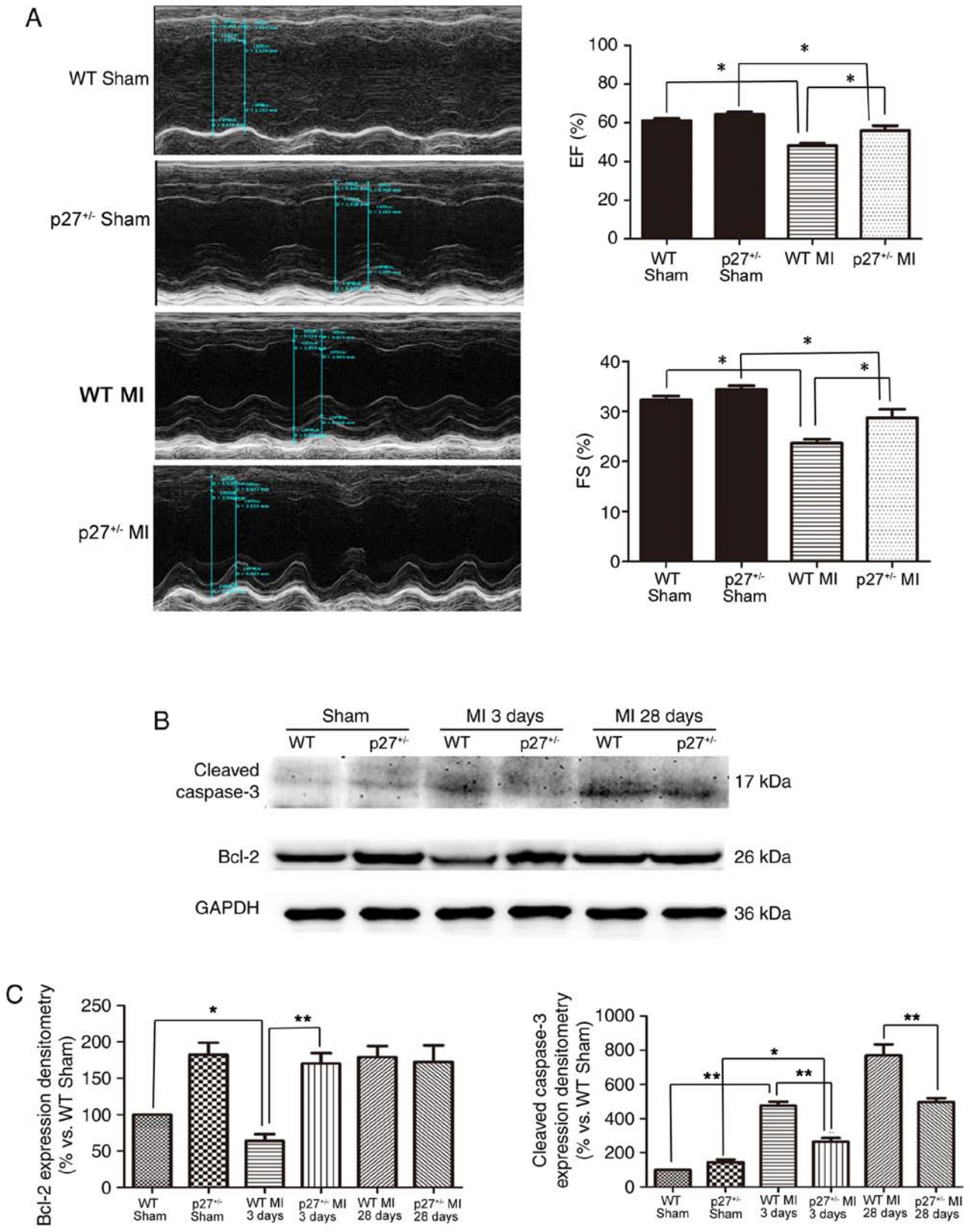

Figure 1. Effects of p27 haploinsufficiency on post-infarction cardiac function and myocardial apoptosis. (A) Representative motion-mode echocardiograms from WT and $p27^{+/-}$ mice at 28 days after sham or MI operations; n=10 mice/group. (B) Representative western blotting of cleaved-caspase 3 and Bcl-2 protein expression in the left ventricle of $p27^{+/-}$ and WT mice at 3 and 28 days after a sham or MI operation; GAPDH served as the loading control. (C) Quantitative analysis of western blotting; n=3. *P<0.05; **P<0.01. EF, ejection fraction; FS, fractional shortening; MI, myocardial infarction; p27, $p27^{kip1}$; WT, wild-type.

artery ligation. It was observed that in both the Sham and MI groups at 28 days the autophagy marker LC3 was expressed at significantly higher levels in the $p27^{+/-}$ groups compared with expression levels in the WT group (P<0.01; Fig. 2A and B).

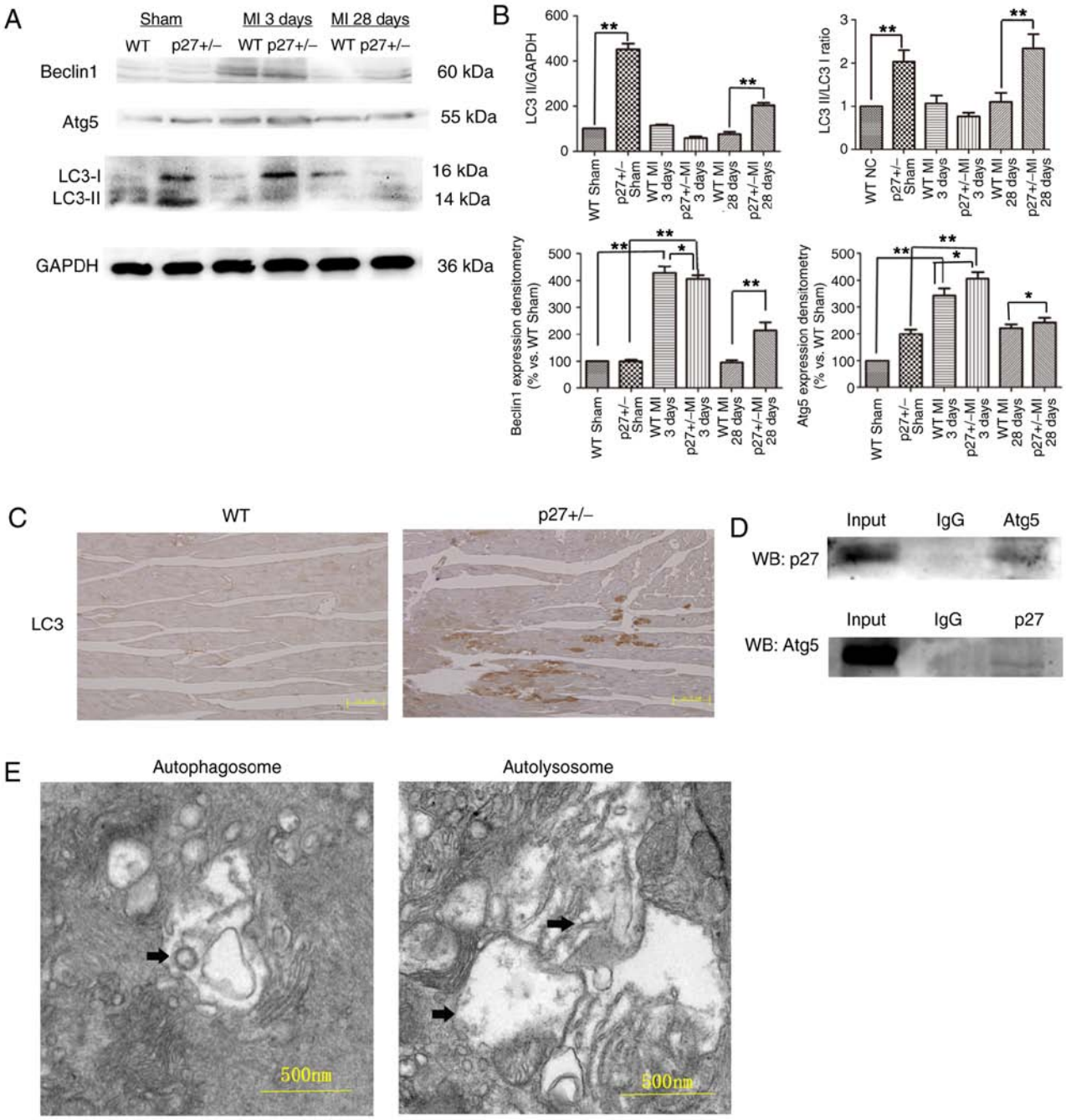

Figure 2. Effects of p27 haploinsufficiency on the expression of autophagy markers in MI hearts. (A) Representative western blots and (B) quantitative analysis of LC3, Beclin 1 and Atg5 protein expression levels in the left ventricle of $p27^{+/-}$ or WT mice at 3 and 28 days after sham or MI operations; GAPDH served as the loading control; n=3; *P<0.05; **P<0.01. (C) LC3 expression in cardiomyocytes in WT and $p27^{+/-}$ mouse hearts after MI operations. (D) Representative co-immunoprecipitation western blots of Atg5 in heart tissue lysates precipitated using p27 antibody, and western blotting of p27 in heart tissue lysates precipitated using Atg5 antibody. (E) Autophagosomes and autolysosomes visualized using transmission electron microscopy 28 days after MI in WT mice. Atg5, autophagy protein 5; LC3, microtubule-associated proteins 1A/1B light chain; MI, myocardial infarction; p27, $p27^{kip1}$; WT, wild-type.

In addition, Beclin 1 and downstream Atg5 expression levels were affected. Beclin 1 was expressed at significantly higher levels in the $p27^{+/-}$ and WT MI groups compared with expression levels in the respective $p27^{+/-}$ Sham and WT MI groups at 3 days (P<0.01), and at 28 days Beclin 1 expression was significantly higher in the $p27^{+/-}$ MI group compared with the WT MI 28 days group (P<0.01) (Fig. 2A and B). Atg5 was also expressed at significantly higher levels in the $p27^{+/-}$ groups compared with expression levels in the respective WT groups (P<0.05 or P<0.01; Fig. 2A and B). These data suggested that p27 haploinsufficiency contributes to the observed increased levels of autophagy in the Sham and MI groups. Furthermore, IHC was used to detect the levels of LC3 in WT and $p27^{+/-}$ mice at 28 days post-surgery; fewer LC3-positive areas were observed in the WT mice compared with the $p27^{+/-}$ mice (Fig. 2C). Co-IP experiments were performed on WT mouse heart tissue lysates. Binding was detected between Atg5 and p27 in heart tissue (Fig. 2D). In addition, TEM also detected the formation of autophagosomes and autolysosomes in WT tissue 28 days after MI (Fig. 2E). These results suggested

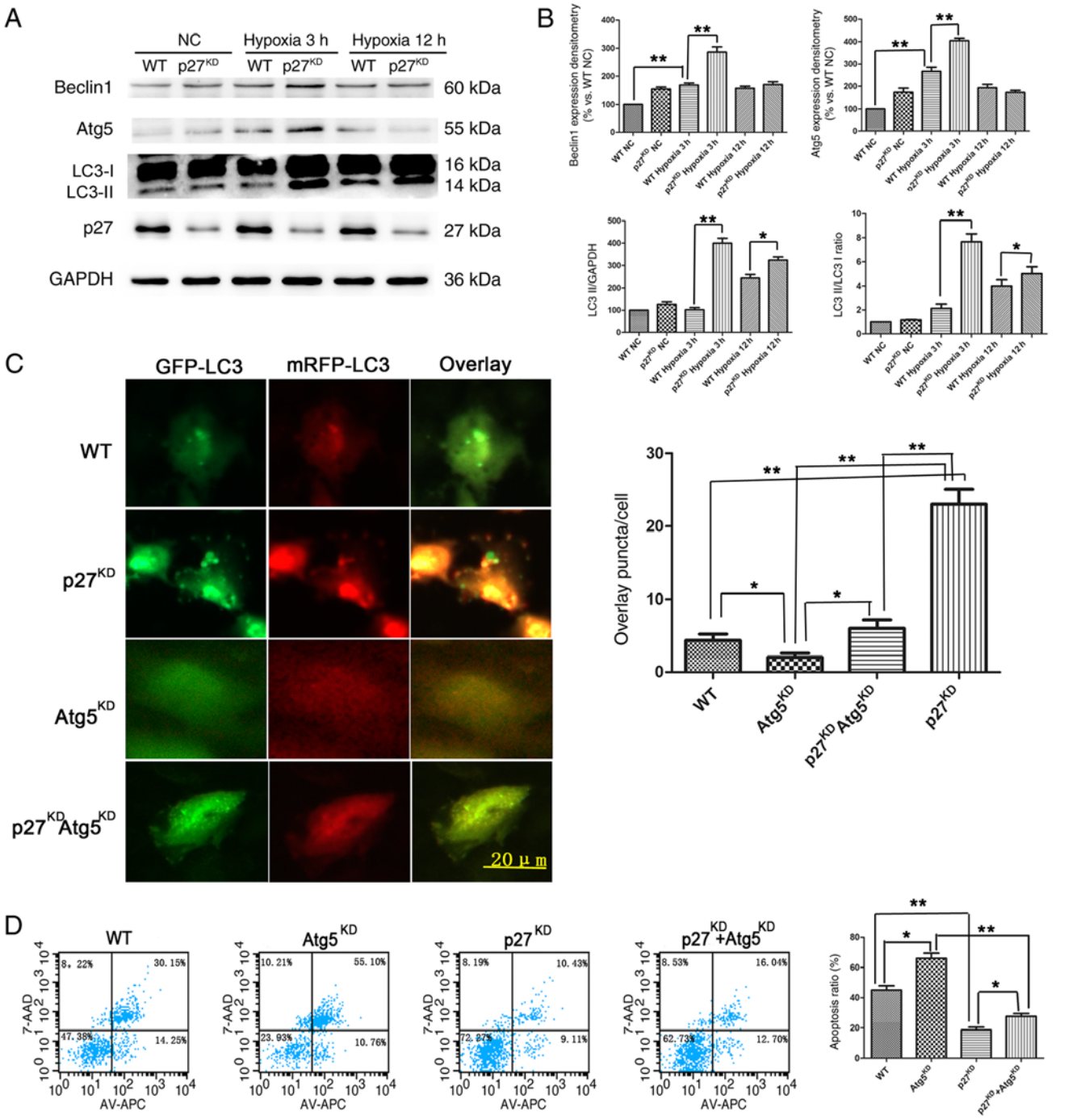

Figure 3. Effects of $p27^{KD}$ on the expression of autophagy markers in H9c2 cells under ischemia/hypoxia. (A) Representative western blotting and (B) quantitative analysis of Beclin 1, Atg5, LC3 and p27 protein expression levels in H9c2 cells exposed for various times to ischemic/hypoxic conditions; GAPDH served as a loading control; n=3. (C) H9c2 cells transfected with mRFP-GFP-LC3 adenovirus and exposed to hypoxic/ischemic conditions for 3 h, the ratio of GFP to mRFP puncta/cell was calculated. (D) Representative plots of apoptotic cardiomyocytes using flow cytometry, quantification is shown as total apoptosis. $^{*}P<0.05$; $^{**}P<0.01$. Atg5, autophagy protein 5; GFP, green fluorescent protein; KD, knockdown; LC3, microtubule-associated proteins 1A/1B light chain; mRFP, monomeric red fluorescent protein; NC, negative control; p27, $p27^{kip1}$.

that p27 haploinsufficiency attenuated ischemic injury by mitigating apoptosis via Atg5-related autophagy.

$p27^{KD}$ restores autophagy flux in the early stages of hypoxia/ischemia in vitro. The lentiviral-mediated stable $p27^{KD}$ H9c2 cell line (~50% efficiency; Fig. S1D) was used to mimic the effect of hypoxia/ischemia in cardiomyocytes. Western blotting was used to determine the expression of the autophagy-related proteins Beclin 1, Atg5 and LC3 in H9c2 cells. The results demonstrated that both Beclin 1 and Atg5 expression were higher in the $p27^{KD}$ H9c2 cells compared with WT cells after 3 h of hypoxia/ischemia, but attenuated after 12 h (Fig. 3A and B). The ratio of LC3-II/I, a hallmark of autophagosomes, coincided with the expression of Beclin 1 and Atg5 (Fig. 3B). Western blotting revealed that after 3 h of hypoxia/ischemia, Beclin 1 and Atg5 protein expression levels increased to a peak expression level compared with WT NC ($P<0.01$), and the levels in $p27^{KD}$ with 3 h of hypoxia were

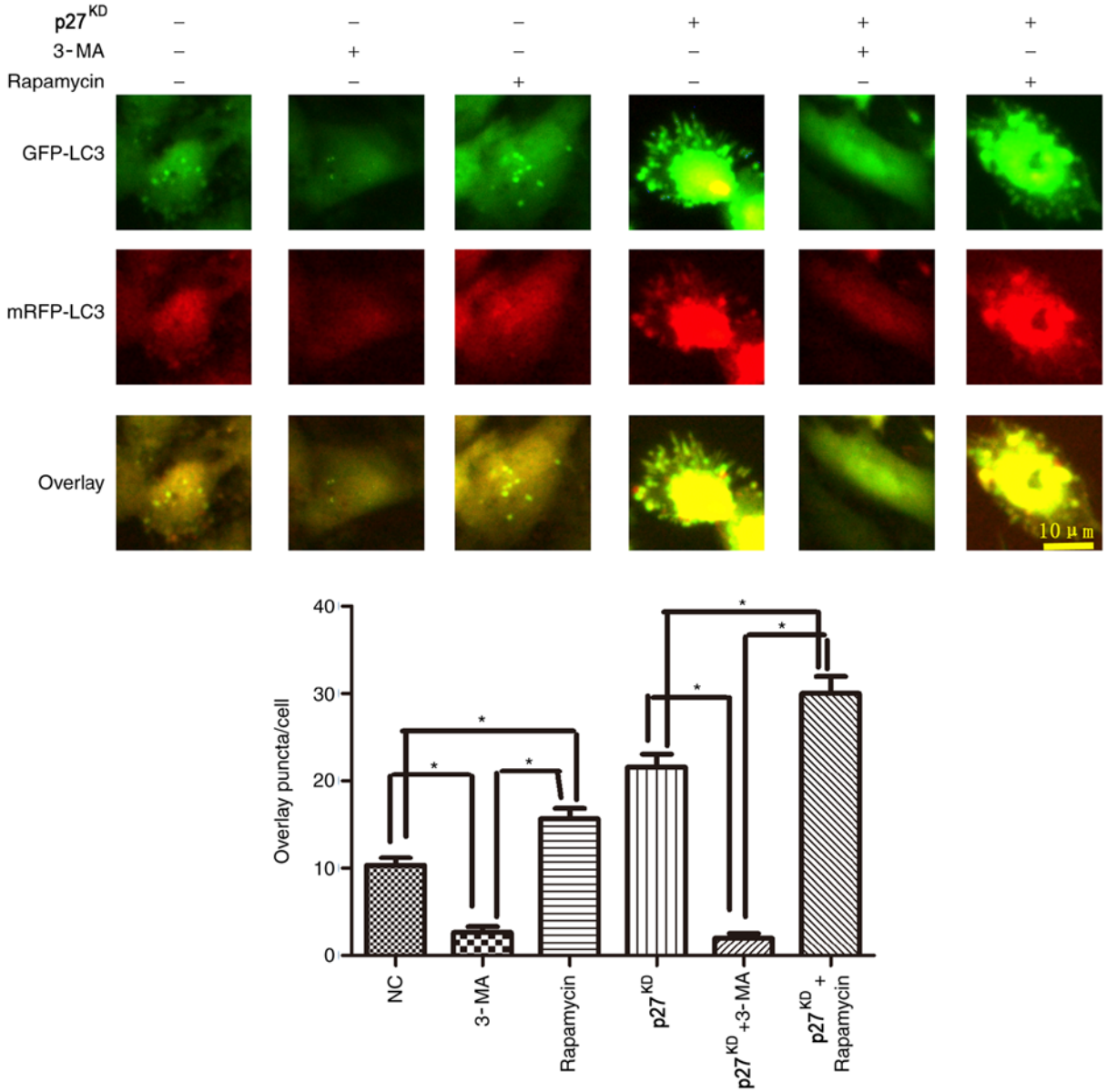

Figure 4. Rapamycin results in increases in GFP and mRFP puncta/cell, whereas 3-MA treatment significantly attenuates the increase in GFP and mRFP puncta/cell. p27 regulated autophagic vesicle-associated-form of LC3II following treatment with rapamycin or 3-MA with 3 h in hypoxic conditions. *P<0.05. 3-MA, 3-methyladenine; GFP, green fluorescent protein; KD, knockdown; LC3, microtubule-associated proteins 1A/1B light chain; mRFP, monomeric red fluorescent protein; p27, $p27^{kip1}$.

significantly higher compared with WT with 3 h of hypoxia (P<0.01) (Fig. 3A and B). H9c2 cells were infected with the mRFP-GFP-LC3 adenovirus and then exposed to 3 h of hypoxia; the results demonstrated that, after 3 h, there was a significantly increased ratio of GFP and mRFP puncta per cell in $p27^{KD}$ cells compared with WT (P<0.01; Fig. 3C), whereas the effects were reversed by $Atg5^{KD}$ co-knockdown (P<0.01; Fig. 3C). Flow cytometry results revealed that total early+late apoptotic rates in $Atg5^{KD}$ cells were significantly increased after 12 h of hypoxia and serum deprivation compared with WT cells (P<0.05; Fig. 3D). $p27^{KD}$ cells had lower apoptosis compared with WT (P<0.01), and co-knockdown of Atg5 reversed this effect of p27 haploinsufficiency (P<0.05). These data indicated that the mechanisms by which p27 insufficiency protects against hypoxia/ischemia may be through restoring the autophagy flux.

p27-mediated autophagy flux is affected by 3-MA/rapamycin. To further investigate whether $p27^{KD}$ improved autophagy flux, cells were treated with the autophagy promoter rapamycin and the autophagy inhibitor 3-MA. Rapamycin treatment resulted in an increased level of GFP and mRFP puncta/cell compared with untreated cells, whereas 3-MA treatment significantly decreased the number of puncta/cell (Fig. 4). In addition, $p27^{KD}$ increased expression of the autophagic vesicle-associated form of LC3II following either rapamycin after 3 h of hypoxia/ischemia (P<0.05; Fig. 4).

Discussion

Myocardial infarction is induced by cardiac coronary vascular and branch occlusion, resulting in nutrient and oxygen insufficiency (21,22). As a result, the ischemic myocardium dies

and is replaced by fibrotic scar tissue (23). Fibroblast cells are implicated in the dysfunction of contractility, leading to heart failure (24). Furthermore, in cardiomyocytes, our previous study reported that 3 and 28 days of hypoxia *in vivo,* and 3 and 12 h of hypoxia *in vitro* induces ischemia/hypoxia that can be used to mimic the early stages of natural heart attack, according to immunodetection and ultrasonic cardiograms (9). Recently, an association between autophagy and cardiac disorders such as myocardial infarction has been demonstrated (25). p27 is a potent cell cycle inhibitor implicated in survival, proliferation, antiapoptotic functions and migration (10). Cardiomyocytes undergo ischemia in the early stages of MI, and $p27^{KD}$ may activate immunoreactivity and autophagy. It has been hypothesized that by promoting the cell cycle, p27 haploinsufficiency could improve cell survival and basic autophagy naturally (26). Previously, it was reported that the knockdown of p27 preserved cardiac function in the early stage of MI by regulating VEGF and HGF, and their receptors, promoting cardiomyocyte survival and leading to proangiogenic effects (9). Similarly, results from the present study demonstrated that $p27^{+/-}$ mice exhibited improved cardiac function and higher cardiomyocyte viability following acute MI compared with WT mice. The reduced survival found in $p27^{-/-}$ mice in the earliest stages after MI, but not in WT and $p27^{+/-}$ mice, has also been described (9). The present study revealed that $p27^{+/-}$ mice had augmented autophagy in the early stages after MI.

Autophagy can be stimulated by various forms of cellular stress, including serum withdrawal, nutrient deprivation, damaged organelles, hypoxia, DNA damage and protein misfolding, which resist apoptosis and necrosis (27,28). Proper autophagy levels are required to maintain cell homeostasis and function. In the heart, uncontrolled autophagy has been demonstrated to contribute to pathological cardiac remodeling and subsequent heart failure (18). Although p27 has been reported to be involved in regulating the process of autophagy (20), few studies have investigated the relationship between p27 and autophagy in the heart. In the present study, it was found that $p27^{KD}$ in cardiomyocytes increased LC3 protein expression *in vivo* and *in vitro*. Furthermore, restored autophagy flux in $p27^{KD}$ ischemic H9C2 cells were observed by GFP/mRFP LC3 fluorescence and IHC. Therefore, the results indicated that p27 may inhibit the autophagy process of cardiomyocytes in the early stages after MI, which may lead to subsequent cardiac dysfunction. In addition, to evaluate the potential contribution of changes in the autophagic flux in $p27^{KD}$ cardiomyocytes, the tandem fluorescence reporter mRFP-GFP-LC3 was used to measure flux. The data from the present study revealed a significantly increased number of GFP and mRFP puncta/cell ratios in $p27^{KD}$ cells, indicating that flux is blocked in the early stages of MI.

Atg5 is an important upstream mediator of autophagy through its binding to LC3, which blocks the formation of autophagosomes (26). It has also been found to serve an important role in the maintenance of cardiac function (29). In the present study, co-IP using Atg5 was used to analyze the relationship between Atg5 and LC3. The results demonstrated that p27 can bind to the Atg5 protein in cardiomyocytes. $p27^{KD}$ increased Atg5 expression and promoted autophagy in the early stages of MI. Furthermore, it was found that $Atg5^{KD}$ reversed the effects of increased autophagy and prevented apoptosis in cultured cardiomyocytes that underwent hypoxia/ischemia. Pathways such as AMP-activated protein kinase/mTOR/ErB/AKT regulate autophagy and apoptosis in cardiomyocytes (16); however, a limited number of studies have attempted to reveal a relationship with p27. The results from the present study provide a new insight of autophagy and apoptosis in cardiomyocytes under hypoxic/ischemic conditions and indicate mechanisms of immunologic injury protection and autophagy flux restoration. The present study indicated that p27 may serve as an inhibitor of Atg5-mediated autophagy activation.

In conclusion, the results from the present study revealed that the p27/Atg5/LC3 pathway modulates the regulation of autophagy in cardiomyocytes under hypoxic/ischemic conditions, providing an insight into the regulation of cardiomyocyte autophagy through p27. The present study paves the way for further studies investigating therapeutic targets of p27 in the early stages of MI.

Acknowledgements

Not applicable.

Funding

The present study was granted financial support from a project supported by the National Natural Science Foundation of China (grant nos. 81670328, 81441011 and 81570328).

Availability of data and materials

All data generated or analyzed during the present study are included in this published article.

Authors' contributions

NZ and JW wrote the manuscript and edited the figures. NZ, WC, QH, JW, DL and YG carried out the molecular laboratory work and participated in the data analysis. DL and QH revised the manuscript and acquired funding. DL, JW and YG supervised all experimental process. QH prepared the supplementary data.

Ethics approval and consent to participate

The protocols of the present study were approved by the Ethics Review of Lab Animal Use Application of Nanjing Medical University (Nanjing, China), and the procedures complied with the National Institutes of Health Guide for the Care and Use of Laboratory Animals.

Patient consent for publication

Not applicable.

Competing interests

The authors declare that they have no competing interests.

References

1. Saleh M and Ambrose JA: Understanding myocardial infarction. F1000Res 7: F1000, 2018.

2. Magnoni M, Berteotti M, Norata GD, Limite LR, Peretto G, Cristell N, Maseri A and Cianflone D: Applicability of the 2013 ACC/AHA risk assessment and cholesterol treatment guidelines in the real world: Results from a multiethnic case-control study. Ann med 48: 282-292, 2016.
3. Ramanathan K, Abel JG, Park JE, Fung A, Mathew V, Taylor CM, Mancini GBJ, Gao M, Ding L, Verma S, *et al*: Surgical versus percutaneous coronary revascularization in patients with diabetes and acute coronary syndromes. J Am Coll Cardiol 70: 2995-3006, 2017.
4. Scimia MC, Gumpert AM and Koch WJ: Cardiovascular gene therapy for myocardial infarction. Expert Opin Biol Ther 14: 183-195, 2014.
5. Wang N, Tong G, Yang J, Zhou Z, Pan H, Huo Y, Xu J, Zhang X, Ling F and Li P: Effect of hepatocyte growth-promoting factors on myocardial ischemia during exercise in patients with severe coronary artery disease. Int Heart J 50: 291-299, 2009.
6. Shen J, Xie Y, Liu Z, Zhang S, Wang Y, Jia L, Wang Y, Cai Z, Ma H and Xiang M: Increased myocardial stiffness activates cardiac microvascular endothelial cell via VEGF paracrine signaling in cardiac hypertrophy. J Mol Cell Cardiol 122: 140-151, 2018.
7. Kaminsky SM, Rosengart TK, Rosenberg J, Chiuchiolo MJ, Van de Graaf B, Sondhi D and Crystal RG: Gene therapy to stimulate angiogenesis to treat diffuse coronary artery disease. Human Gene Ther 24: 948-963, 2013.
8. Zhao Q, Huang J, Wang D, Chen L, Sun D and Zhao C: Endothelium-specific CYP2J2 overexpression improves cardiac dysfunction by promoting angiogenesis via Jagged1/Notch1 signaling. J Mol Cell Cardiol 123: 118-127, 2018.
9. Zhou N, Fu Y, Wang Y, Chen P, Meng H, Guo S, Zhang M, Yang Z and Ge Y: p27(kip1) haplo-insufficiency improves cardiac function in early-stages of myocardial infarction by protecting myocardium and increasing angiogenesis by promoting IKK activation. Sci Rep 4: 5978, 2014.
10. Koff A and Polyak K: p27KIP1, an inhibitor of cyclin-dependent kinases. Prog Cell Cycle Res 1: 141-147, 1995.
11. Li Y, Ding X, Fan P, Guo J, Tian X, Feng X, Zheng J, Tian P, Ding C and Xue W: Inactivation of p27(kip1) promoted nonspecific inflammation by enhancing macrophage proliferation in islet transplantation. Endocrinology 157: 4121-4132, 2016.
12. Marone M, Bonanno G, Rutella S, Leone G, Scambia G and Pierelli L: Survival and cell cycle control in early hematopoiesis: Role of bcl-2, and the cyclin dependent kinase inhibitors P27 and P21. Leuk Lymphoma 43: 51-57, 2002.
13. Rehman G, Shehzad A, Khan AL and Hamayun M: Role of AMP-activated protein kinase in cancer therapy. Arch Pharm (Weinhim) 347: 457-468, 2014.
14. Rossi A, Kontarakis Z, Gerri C, Nolte H, Holper S, Kruger M and Stainier DY: Genetic compensation induced by deleterious mutations but not gene knockdowns. Nature 524: 230-233, 2015.
15. Deter RL, Baudhuin P and De Duve C: Participation of lysosomes in cellular autophagy induced in rat liver by glucagon. J Cell Biol 35: C11-C16, 1967.
16. Wang Y, Liu J, Tao Z, Wu P, Cheng W, Du Y, Zhou N, Ge Y and Yang Z: Exogenous HGF prevents cardiomyocytes from apoptosis after hypoxia via up-regulating cell autophagy. Cell Physiol Biochem 38: 2401-2413, 2016.
17. Dai SN, Hou AJ, Zhao SM, Chen XM, Huang HT, Chen BH and Kong HL: Ginsenoside Rb1 ameliorates autophagy of hypoxia cardiomyocytes from neonatal rats via AMP-activated protein kinase pathway. Chin J Integr Med 25: 521-528, 2019.
18. Ponnusamy M, Li PF and Wang K: Understanding cardiomyocyte proliferation: An insight into cell cycle activity. Cell Mol Life Sci 74: 1019-1034, 2017.
19. Ding Y, Kim JK, Kim SI, Na HJ, Jun SY, Lee SJ and Choi ME: TGF-{beta}1 protects against mesangial cell apoptosis via induction of autophagy. J Biol Chem 285: 37909-37919, 2010.
20. Sun X, Momen A, Wu J, Noyan H, Li R, von Harsdorf R and Husain M: p27 protein protects metabolically stressed cardiomyocytes from apoptosis by promoting autophagy. J Biol Chem 289: 16924-16935, 2014.
21. Arya R and White K: Cell death in development: Signaling pathways and core mechanisms. Semin Cell Dev Biol 39: 12-19, 2015.
22. Stegehuis VE, Wijntjens GW, Piek JJ and van de Hoef TP: Fractional flow reserve or coronary flow reserve for the assessment of myocardial perfusion: Implications of FFR as an imperfect reference standard for myocardial ischemia. Curr Cardiol Rep 20: 77, 2018.
23. Lopez B, Gonzalez A, Ravassa S, Beaumont J, Moreno MU, San Jose G, Querejeta R and Diez J: Circulating biomarkers of myocardial fibrosis: The need for a reappraisal. J Am Coll Cardiol 65: 2449-2456, 2015.
24. Delgado V, van Bommel RJ, Bertini M, Borleffs CJ, Marsan NA, Arnold CT, Nucifora G, van de Veire NR, Ypenburg C, Boersma E et al: Relative merits of left ventricular dyssynchrony, left ventricular lead position, and myocardial scar to predict long-term survival of ischemic heart failure patients undergoing cardiac resynchronization therapy. Circulation 123: 70-78, 2011.
25. Sun T, Li MY, Li PF and Cao JM: MicroRNAs in cardiac autophagy: Small molecules and big role. Cells 7: E104, 2018.
26. Li H, Peng X, Wang Y, Cao S, Xiong L, Fan J, Wang Y, Zhuang S, Yu X and Mao H: Atg5-mediated autophagy deficiency in proximal tubules promotes cell cycle G2/M arrest and renal fibrosis. Autophagy 12: 1472-1486, 2016.
27. Booth LA, Tavallai S, Hamed HA, Cruickshanks N and Dent P: The role of cell signalling in the crosstalk between autophagy and apoptosis. Cell Signal 26: 549-555, 2014.
28. Kaminskyy VO and Zhivotovsky B: Free radicals in cross talk between autophagy and apoptosis. Antioxid Redox Signal 21: 86-102, 2014.
29. Huang WQ, Wen JL, Lin RQ, Wei P and Huang F: Effects of mTOR/NF-κB signaling pathway and high thoracic epidural anesthesia on myocardial ischemia-reperfusion injury via autophagy in rats. J Cell Physiol 233: 6669-6678, 2018.